Spectrochimica Acta Part A 75 (2010) 1370–1376

Contents lists available at ScienceDirect

Spectrochimica Acta Part A: Molecular and Biomolecular Spectroscopy

journal homepage: www.elsevier.com/locate/saa

Theoretical and vibrational studies of 4,5-diphenyl-2-2 oxazole propionic acid (oxaprozin)

Seda G. Sagdinc[a,*], Aslı Esme[b]

[a] Department of Physics, Kocaeli University, Umuttepe Campus, 41380 Kocaeli, Turkey
[b] Department of Elementary Science Education, Kocaeli University, Umuttepe Campus, 41380 Kocaeli, Turkey

ARTICLE INFO

Article history:
Received 20 November 2009
Accepted 15 January 2010

Keywords:
Oxaprozin
DFT
HF
FT-IR
FT-Raman
Hyperpolarizability

ABSTRACT

The molecular structure, linear and nonlinear optical properties, and electronic properties of 4,5-diphenyl-2-2 oxazole propionic acid (oxaprozin) as a monomer were investigated by using Hartree–Fock (HF) and density functional theory (DFT) calculations that used 6-31G(d,p) basis set. The first-order hyperpolarizability of oxaprozin (OXA) was found to be 1.117×10^{-30} esu. The structure of oxaprozin dimer with HF/6-31G(d) level caused by the shifts of O–H and C=O bands in the vibrational spectra of oxaprozin were also studied. Moreover, these calculated frequencies of oxaprozin dimer were compared with the solid FT-IR and FT-Raman spectra. The theoretical frequencies and infrared intensities were showed a good agreement with experimental data.

1. Introduction

Oxaprozin, chemically known as 4,5-diphenyl-2-2 oxazole propionic acid, OXA, is one of the widely used non-steroidal anti-inflammatory drugs (NSAIDs) that are therapeutically used in inflammatory and painful diseases of rheumatic and non-rheumatic origin [1]. It was the first representative member of the diaryl substituted heterocyclic COX-2 inhibitor currently practiced [2]. OXA chemically differs from other propionic acid compounds since the propionic acid group attached to the oxazole does not posses a chiral centre [3].

The organic molecules, for use in devices, are of recent interest because their nonlinear optical (NLO) responses are orders of magnitude larger than those of conventional inorganic crystals. Porphyrins, phthalocyanines, aromatic, and mesoionic complexes are examples of organic compounds intensively investigated due to their NLO properties [4]. Several methodologies including semi empirical, ab initio, and density functional theory (DFT) have been employed for the calculation of NLO properties of the organic molecules in the recent years [5–8]. Diclofenac sodium, one of the NSAIDs, was examined by means of the linear and nonlinear optical properties by using the Hartree–Fock (HF) and DFT methods with several basis sets [8]. According to that study, the HF level of theory, using the medium basis set 6-31G(d,p) extended with p and d polarized functions, was the best suited one for the description of such an electrical property.

More recently, the vibrational properties and theoretical investigation of flurbiprofen and fenbufen, known as NSAIDs, by using quantum chemical calculations were studied by the authors of this paper [9,10]. This present work constitutes a development of these studies and is a continuation of the previously mentioned recent spectroscopic and theoretical study of vibrational spectra of some NSAIDs [9–12]. No detailed spectroscopic and harmonic vibrational frequency calculations for OXA have been reported and analyzed in the literature up to the present. Therefore, this investigation was undertaken to completely study the vibrational spectra of the molecule. Ab initio HF/6-31G(d) calculation of OXA dimer was performed to support the wavenumber assignments. Furthermore, the molecular structure, electronic, and optical properties (polarizability (α) and hyperpolarizability (β)) of OXA was studied by using HF and B3LYP methods. The results of this study might have useful predictive value and can be of direct interest for understanding nonlinear optical properties of higher organic systems considering the lack of both experimental and theoretical β determinations.

2. Spectroscopic measurements

Oxaprozin in solid form was purchased from the Sigma–Aldrich Chemical Company (USA), with a stated purity of greater than 98% and it was used without further purification. The FT-IR spectrum was recorded on a Bruker Alpha-P spectrometer equipped with ATR platinum Diamond. The FT-Raman spectrum (in the 3500–10 cm^{-1}

* Corresponding author. Tel.: +90 2623032047.
E-mail address: seda.sagdinc@gmail.com (S.G. Sagdinc).

1386-1425/$ – see front matter © 2010 Elsevier B.V. All rights reserved.
doi:10.1016/j.saa.2010.01.004

region) of solid oxaprozin, on the other hand, was measured on a Jobin Yvon LabRam confocal microscopy Raman spectrometer with a charge coupled device (CCD) detector and a holographic notch filter. The spectrograph was equipped with an 1800-grooves/mm grating; and measurement was performed with a 200-m entrance slit. Excitation source was provided by 632.8 nm of He–Ne laser with 20 mW at the sample. Sample was maintained at ambient temperature (20 °C) during the spectral scan.

3. Calculations

Experimental molecular geometry of OXA monomer was used as the initial guess for geometry optimization. The molecular structure of OXA monomer in the ground state (in vacuo) was optimized by B3LYP [13,14] and HF method using 6-31G(d,p) basis set. Moreover, the molecular structure of OXA as a dimer was studied by using HF/6-31G(d) basis set. Vibrational frequencies calculated at same level were then scaled by 0.8929 [15]. The calculations were accomplished with GAUSSIAN 03 (Revision B.05) [16] and GAUSSIAN 03W [17].

In this paper, we are presented values of mean polarizability, α, as defined in the following equation:

$$\bar{\alpha} = \frac{1}{3}(\alpha_{xx} + \alpha_{yy} + \alpha_{zz}) \quad (1)$$

and sometimes the anisotropy ($\Delta\alpha$) which is written here in an obvious notation as

$$\Delta\alpha = \left\{ \frac{(\alpha_{xx} - \alpha_{yy})^2 + (\alpha_{xx} - \alpha_{zz})^2 + (\alpha_{zz} - \alpha_{yy})^2}{2} \right\}^{1/2} \quad (2)$$

The first hyperpolarizability (β) reported here is defined as

$$\beta_{\text{total}} = [(\beta_{xxx} + \beta_{xyy} + \beta_{xzz})^2 + (\beta_{yyy} + \beta_{yzz} + \beta_{yxx})^2 + (\beta_{zzz} + \beta_{zxx} + \beta_{zyy})^2]^{1/2} \quad (3)$$

The α and β components of GAUSSIAN 03W output were reported in atomic units, thus, the calculated values had to be converted into electrostatic units (α: 1 a.u. = 0.1482×10^{-24} esu; β: 1 a.u. = 8.6393×10^{-33} esu) [18].

4. Results and discussion

4.1. Geometric parameters

The closed molecular formula of the oxaprozin (OXA) is $C_{18}H_{15}NO_3$. Due to the fact that the structure of this molecule has been previously reported in the literature, we first investigated this molecule as a monomer [19]. The geometry of monomer structure was determined at the B3LYP and HF levels of theory employing 6-31G(d,p) basis set. The crystal structure [19] and B3LYP/6-31G(d,p) optimized structure of OXA molecule are shown in Fig. 1.

The calculated geometric parameters at HF and DFT methods with B3LYP/6-31G(d,p) levels for OXA monomer were compared with the experimental parameters [19] in Table 1. As can be seen, there was a good agreement between experimental and the calculated geometric parameters. The major discrepancy was noted by C–O bond length. The investigation of the X-ray structures revealed that the C–O distance values were in a range from 1.303 to 1.345 Å [9,10,20] in other NSAIDs. Although the experimental C(20)–O(2) C–O bond length is 1.226 Å for OXA monomer, this value was calculated as 1.328 and 1.332 Å, respectively, by using HF and B3LYP methods. The B3LYP method provides systematic longer bonds with respect to HF method as can be seen from Table 1. Moreover, the largest discrepancies of bond angles were observed for the angles that corresponded to the oxygen atoms in the carboxylic group.

For the monomer structure of OXA, the discrepancy between the experimental and calculated values for the atomic coordinates

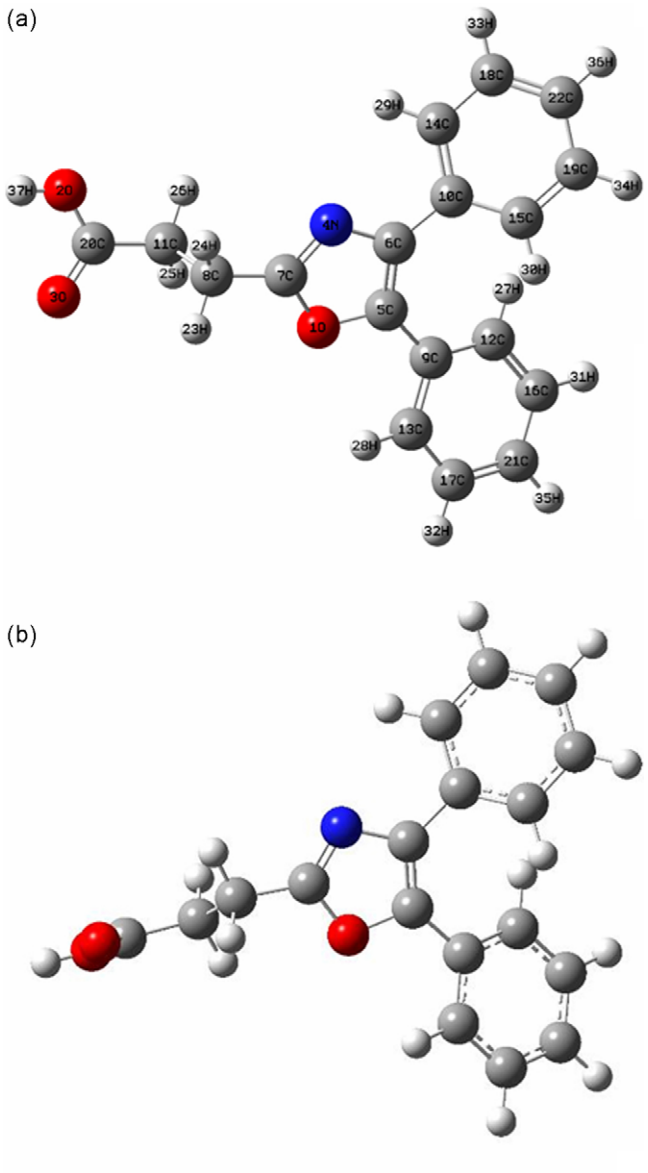

Fig. 1. (a) Crystal structure [19] and (b) optimized structure obtained using B3LYP/6-31G(d,p) of OXA.

might result from the different environments of a molecule in the experimental crystalline state and in the theoretical gas phase. The calculated bond lengths and angles represent a good approximation in spite of these differences; and they became the basis for calculating other parameters, such as vibrational frequencies and polarizability properties, as described below.

Secondly, molecular geometric parameter of purposed OXA dimer was also investigated by using HF/6-31G(d) level (Fig. 2). The molecular structure of OXA dimer forms an intermolecular hydrogen bond between the two oxygen atoms of the carboxyl group for the OXA monomer. The optimized bond lengths and angles for dimer form are also presented in Table 1. The hydrogen bond length O(1)...O(2′) of OXA was found as 2.721 Å. Boczar et al. also calculated this bond length as 2.643 Å for aspirin [20] by using B3LYP/6-31++G** level. This bond length was also observed to be 2.649 Å [20] and 2.64 Å [21] for aspirin and flurbiprofen, respectively. The O...H...O angle of 168.8° was the shortest among the NSAIDs with dimer structure (173.8° for aspirin, 178.1° for flurbiprofen).

Table 1
Experimental and optimized geometrical parameters of oxaprozin [bond length (Å),bond angles (°), dihedral angles (°)].

Parameters	Exp[a]	HF[b] 6-31G(d,p)	B3LYP[b] 6-31G(d,p)	HF[c] 6-31G(d)		Exp[a]	HF[b] 6-31G(d,p)	B3LYP[b] 6-31G(d,p)	HF[c] 6-31G(d)
Bond lengths (Å)					Bond angles (°)				
O(2)–C(20)	1.226	1.328	1.332	1.322	O(3)–C(20)–O(2)	118.65	122.60	122.77	122.50
O(3)–C(20)	1.222	1.188	1.211	1.225	O(3)–C(20)–C(11)	120.51	125.67	125.83	121.18
C(20)–C(11)	1.448	1.506	1.513	1.492	O(2)–C(20)–C(11)	120.83	111.73	111.40	113.33
C(11)–C(8)	1.551	1.529	1.536	1.529	C(20)–C(11)–C(8)	111.50	112.20	112.07	112.82
C(8)–C(7)	1.470	1.492	1.491	1.482	C(11)–C(8)–C(7)	111.62	111.92	112.71	111.88
C(7)–N(4)	1.334	1.269	1.295	1.279	C(8)–C(7)–O(1)	124.96	117.91	117.76	118.63
N(4)–C(6)	1.348	1.393	1.397	1.348	C(8)–C(7)–N(4)	125.99	128.33	128.70	129.53
C(6)–C(5)	1.416	1.347	1.377	1.412	C(7)–O(1)–C(5)	108.78	105.84	105.55	106.57
C(5)–O(1)	1.357	1.367	1.384	1.393	O(1)–C(5)–C(6)	106.34	106.77	106.69	106.41
O(1)–C(7)	1.342	1.331	1.361	1.360	C(5)–C(6)–N(4)	106.46	108.31	108.64	108.32
C(6)–C(10)	1.434	1.478	1.472	1.470	C(6)–N(4)–C(7)	109.38	105.30	105.55	106.83
C(10)–C(14)	1.423	1.392	1.405	1.393	N(4)–C(7)–O(1)	109.05	113.77	113.54	111.84
C(5)–C(9)	1.430	1.471	1.462	1.463	C(5)–C(6)–C(10)	134.50	131.73	131.87	132.28
C(9)–C(13)	1.422	1.393	1.407	1.393	N(4)–C(6)–C(10)	119.04	119.96	119.46	119.39
C(13)–C(17)	1.406	1.384	1.393	1.385	C(19)–C(22)–C(18)	119.70	119.61	119.53	119.57
C(17)–C(21)	1.404	1.385	1396.	1.387	C(22)–C(18)–C(14)	119.80	120.24	120.31	120.27
C(21)–C(16)	1.405	1.386	1.397	1.387	C(18)–C(14)–C(10)	121.72	120.52	120.63	120.54
C(16)–C(12)	1.410	1.384	1.393	1.385	C(14)–C(10)–C(15)	117.14	118.87	118.62	118.80
C(12)–C(9)	1.417	1.392	1.407	1.394	C(6)–C(10)–C(15)	123.83	121.78	122.27	121.88
O(2)–H(37)...O(3′)	–	–	–	2.721	C(6)–C(10)–C(14)	119.01	119.33	119.07	119.29
H(37)...O(3′)	–	–	–	1.766	C(6)–C(5)–C(9)	135.43	136.97	137.53	137.51
Dihedral angles (°)					O(1)–C(5)–C(9)	118.23	116.25	115.73	116.06
O(3)–C(20)–C(11)–C(8)	−67.91	−2.85	−6.03	−3.54	C(5)–C(9)–C(12)	124.60	121.09	121.38	121.19
O(2)–C(20)–C(11)–C(8)	112.22	177.39	174.43	176.74	C(5)–C(9)–C(13)	118.33	119.88	119.93	119.81
C(7)–C(8)–C(11)–C(20)	−179.84	178.17	175.99	177.46	C(9)–C(13)–C(17)	121.82	120.44	120.57	120.44
C(11)–C(8)–C(7)–N(4)	84.04	116.96	118.01	121.94	C(13)–C(17)–C(21)	119.76	120.22	120.34	120.24
C(11)–C(8)–C(7)–O(1)	−95.99	−62.96	−62.05	−58.60	C(17)–C(21)–C(16)	119.67	119.66	119.52	119.64
C(7)–O(1)–C(5)–C(9)	−178.83	−177.70	−176.72	−177.44	C(21)–C(16)–C(12)	120.25	120.30	120.44	120.27
C(8)–C(7)–O(1)–C(5)	180.00	179.67	179.76	−179.92	C(16)–C(12)–C(9)	121.21	120.36	120.47	120.41
C(8)–C(7)–N(4)–C(6)	179.84	179.40	179.21	178.77	C(12)–C(9)–C(13)	117.06	119.02	118.66	118.99
C(7)–O(1)–C(5)–C(6)	0.17	1.13	1.21	1.34	O(1)...H(1)...(2′)	–	–	–	168.8

[a] Ref. [19].
[b] OXA.
[c] OXA dimer.

4.2. Electronic properties of OXA

3D plots of HOMO and LUMO of studied molecule are shown in Fig. 3. The highest occupied molecular orbitals (HOMO) and the lowest unoccupied molecular orbitals (LUMO) were localized mainly on oxazole and π-bonds of phenyl rings of OXA molecule. The coefficients of the HOMO and LUMO for OXA using HF/6-31G(d,p) level were calculated as follows:

$$\varphi_{\mathrm{HOMO}}^{\mathrm{OXA}} \approx -0.21 * 1s^{\mathrm{O1}} + 0.28 * 2p_Z^{\mathrm{C5}} + 0.21 * 3p_Z^{\mathrm{C5}} + 0.25 * 2p_Z^{\mathrm{C6}} + 0.18 * 3p_Z^{\mathrm{C6}} - 0.21 * 2p_Z^{\mathrm{C7}} - 0.14 * 3p_Z^{\mathrm{C7}} + 0.17 * 2p_Z^{\mathrm{C22}} \quad (4)$$

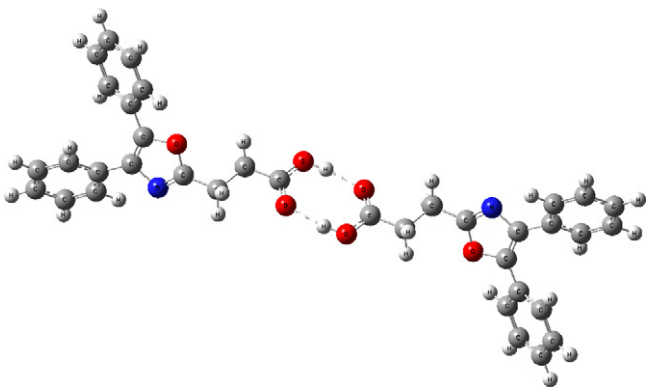

Fig. 2. Geometry of the OXA dimer, optimized at the HF/6-31G(d) level.

$$\varphi_{\mathrm{LUMO}}^{\mathrm{OXA}} \approx -0.20 * 2p_Z^{\mathrm{O1}} - 0.20 * 3p_Z^{\mathrm{O1}} + 0.26 * 2p_Z^{\mathrm{C5}} - 0.23 * 2p_Z^{\mathrm{C6}} - 0.23 * 3p_Z^{\mathrm{C6}} + 0.22 * 2p_Z^{\mathrm{C9}} + 0.21 * 3p_Z^{\mathrm{C21}} - 0.17 * 3p_Z^{\mathrm{C22}} \quad (5)$$

Mulliken's population analysis [22] provides a partitioning of either a total charge density or an orbital density. Atomic charges on the various atoms of OXA monomer obtained by Mulliken population analysis and energies are given in Table 2. From the listed atomic charge values, the oxygen [O(1), O(2) and O(3)] and N(4) atoms had a large negative charge and behaved as electron acceptors. It was found that the most positively charged atoms were C(7) and C(20). It was also observed that there is a large accumulation of positive charge on atom C(20) and negative charge on O(2) in OXA molecule. Therefore, this might had given C(20)–O(2) bond a greater ionic character.

4.3. Polarizabilities and hyperpolarizabilities

In the presence of an applied electric field, the energy of a system is a function of the electric field. The third rank tensor of first hyperpolarizability β is described by a $3 \times 3 \times 3$ matrix. The 27 components of the 3D matrix can be reduced to 10 components due to the Kleinman symmetry [23]. The β components are defined as the coefficients in the Taylor series expansion of the energy in the external electric field. This expansion occurs when the external electric field is weak and homogeneous,

$$E = E_0 - \mu_i F_i - (1/2)\alpha_{ij} F_i F_j - (1/6)\beta_{ijk} F_i F_j F_k - \cdots \quad (6)$$

E is the energy of a molecule under the electric field F; E_0 is the unperturbed energy of a free molecule; F_i is the vector component of the electric field in the i direction; μ_i is the dipole moment; α_{ij} is

Table 2
The Mulliken atomic charges obtained by HF and B3LYP methods with 6-31G(d,p) basis set for the molecule studied.

Atoms	HF 6-31G(d,p)	B3LYP 6-31G(d,p)	Atoms	HF 6-31G(d,p)	B3LYP 6-31G(d,p)
O(1)	−0.744	−0.535	C(12)	−0.168	−0.120
O(2)	−0.732	−0.556	C(13)	−0.169	−0.123
O(3)	−0.554	−0.317	C(14)	−0.174	−0.128
N(4)	−0.548	−0.410	C(15)	−0.181	−0.134
C(5)	0.265	0.167	C(16)	−0.214	−0.145
C(6)	0.030	0.010	C(17)	−0.208	−0.137
C(7)	0.606	0.440	C(18)	−0.209	−0.138
C(8)	−0.322	−0.285	C(19)	−0.212	−0.145
C(9)	0.007	0.072	C(20)	0.236	0.491
C(10)	0.021	0.092	C(21)	−0.187	−0.111
C(11)	−0.146	−0.317	C(22)	−0.189	−0.113

a second rank tensor property called the dipole polarizability; and β_{ijk} is the first of an infinite series of dipole hyperpolarizabilities [24]. Each subscript i, j and k denote the indices of the Cartesian axes x, y and z [25].

The static dipole polarizability, α, is linear response property of a molecule and its importance for the prediction of the molecular interaction effects is well recognized [26]. In case of a molecule, it is very sensitive to basis set, electron correlation and relativistic effects, and the vibrational structure. The components of the (α)-tensor, ($\bar{\alpha}$) and μ are reported in Table 3. The predicted results at the different levels of computations did not differ much. The permanent dipole moment was found to be 2.98 and 2.70 D, respectively, almost independent of the basis set.

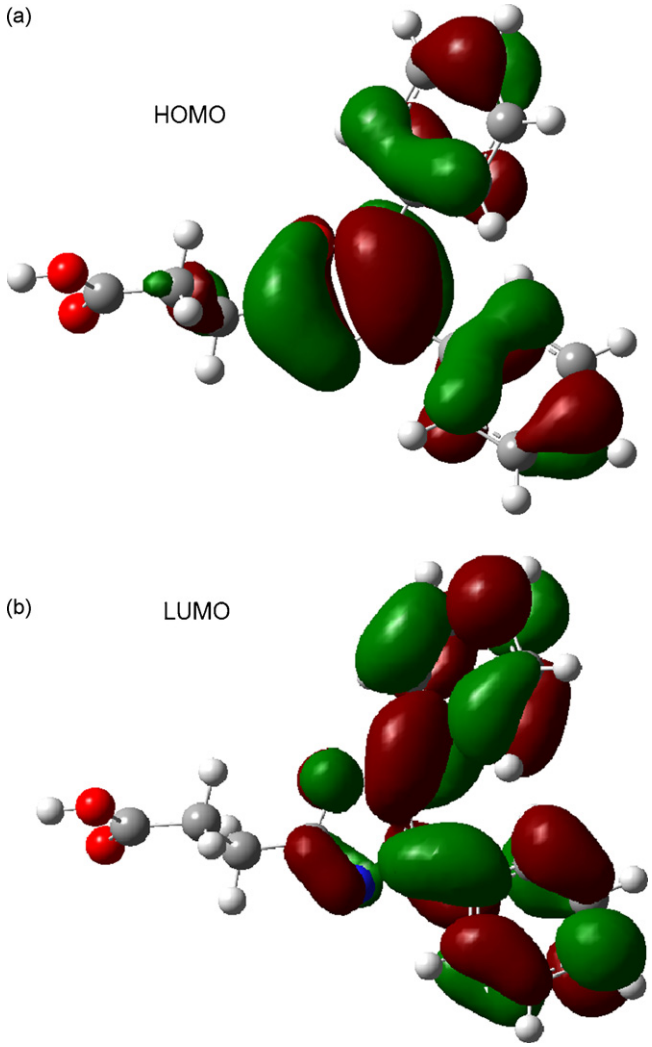

Fig. 3. 3D HOMO and LUMO plots on OXA dimer with HF/6-31G(d,p) level.

The dipole hyperpolarizability is obtained as the second derivative of the energy. The use of more accurate theoretical descriptions for the studied compounds and approximating the theoretical values to the experimental ones tend to improve the estimated value for (β). Otherwise, simulations exclusively based on ab initio and DFT methods are capable to furnish better result in principle. In this study, the polarizability and the first hyperpolarizability was calculated as a numerical derivative of the dipole moment by using B3LYP and HF methods with 6-31G(d,p) basis set (Table 3). The calculated first hyperpolarizabilities of OXA by using HF/6-31G(d,p) and B3LYP/6-31G(d,p) levels; which were found as 1.029×10^{-30} and 1.117×10^{-30} esu, respectively. These values were found nearly five times more than that of urea (0.1947×10^{-30} esu) by using B3LYP 6-31G(d,p) level. Therefore, the title compound was a good candidate as second-order nonlinear optical material.

The non-diagonal component, β_{xxz}, had the largest value among the ten components as can be seen from Table 3. The values of the components were found to be relatively medium in directions of β_{xxy}, β_{xyy}, β_{yyy}, β_{xyz}, and β_{yyz}. The theoretical calculation seemed to be more helpful for determination of particular components of β. Domination of particular components indicates on a substantial delocalization of charges in those directions. It was noticed that in β_{xxx} direction, which is the principal dipole moment axis antiparallel to the charge transfer axis, the smallest values of hyperpolarizability were noticed; and subsequently, electron cloud was more delocalized in the opposite of that direction [27].

Infrared and Raman spectra can be used not only to obtain structural information of molecules but also to evaluate the vibrational contribution β to the molecular hyperpolarizabilities [28,29]. The presence of such vibrational contributions can be inferred from infrared and Raman spectra. The analytic expressions for vibrational hyperpolarizabilities are given by

$$\beta^{v}_{nmp} = \frac{1}{4\pi^2 c^2} \sum_k \frac{1}{V_k} \left[\left(\frac{\partial \mu_n}{\partial Q_k} \right) \left(\frac{\partial \alpha_{mp}}{\partial Q_k} \right) + \left(\frac{\partial \mu_m}{\partial Q_k} \right) \left(\frac{\partial \alpha_{np}}{\partial Q_k} \right) + \left(\frac{\partial \mu_p}{\partial Q_k} \right) \left(\frac{\partial \alpha_{np}}{\partial Q_k} \right) \right] \quad (7)$$

where V_k are vibrational frequencies; and $\partial\mu/\partial Q_k$, $\partial\alpha/\partial Q_k$, and $\partial\beta/\partial Q_k$ are derivatives of the molecular dipole moment and polarizabilities, respectively, in regards to kth normal coordinate while the sum extends over all vibrational normal modes [30,31]. These parameters can be obtained from infrared intensities and Raman and Raman cross sections, respectively.

The potential application of OXA in the field of nonlinear optics demands the investigation of the contribution of IR and Raman active vibrational modes to the hyperpolarizability enhance-

Table 3
Components of first-order hyperpolarizability (β) and molecular dipole polarizability (a.u.) converged mean and anisotropic polarizabilities ($\langle\alpha\rangle$, a.u.), and dipole moments (Debye) of the 4,5-diphenyl-2-2 oxazole-propionic acid.

	HF 6-31G(d,p)	B3LYP 6-31G(d,p)		HF 6-31G(d,p)	B3LYP 6-31G(d,p)		HF 6-31G(d,p)	B3LYP 6-31G(d,p)
β_{xxx}	−80.0743	−93.3058	α_{xx}	−112.3777	−109.6161	μ_x	1.2057	0.4225
β_{xxy}	16.8594	14.3480	α_{xy}	−2.7186	−2.2435	μ_y	2.2356	1.8265
β_{xyy}	15.6612	11.4102	α_{yy}	−119.9638	−118.1837	μ_z	1.5575	1.9441
β_{yyy}	29.2606	22.2404	α_{yz}	−7.4393	−5.5773	μ(D)	2.98	2.70
β_{xxz}	67.5355	66.7492	α_{zz}	−129.0331	−128.0344			
β_{xyz}	15.3223	14.0959	α_{xz}	−6.2413	−5.6614			
β_{yyz}	10.8314	12.2403	$\langle\alpha\rangle$	−120.46	−118.61			
β_{xzz}	−12.3475	−13.5950	$\langle\Delta\alpha\rangle$	14.44	15.02			
β_{yzz}	3.2690	1.5450	$\langle\alpha\rangle \times 10^{-24}$ (esu)	2.14	2.37			
β_{zzz}	−1.8859	−0.5894						
β_{total} (a.u.)	119.083	129.303						
$\beta \times 10^{-30}$ (esu)	1.029	1.117						

ment. The bands at 3056 cm^{-1}, 1568 cm^{-1},1216 cm^{-1},1152 cm^{-1} 1143 cm^{-1}, 1060 cm^{-1}, and 616 cm^{-1} observed in IR have their counterparts in Raman at 3064 cm^{-1}, 1570 cm^{-1}, 1220 cm^{-1}, 1159 cm^{-1}, 1145 cm^{-1}, 1063 cm^{-1}, and 617 cm^{-1}, respectively. Every vibrational mode is not both infrared and Raman active. IR and Raman activities are complementary although it has not of inversion symmetry of OXA. These bands, which are associated to be strongly active simultaneously both in IR and Raman spectra specific modes provide evidence for the charge transfer interaction between the donor and the acceptor group through the π-system [31].

4.4. Experimental and theoretical vibrational spectra of oxaprozin

Based on the previously reported vibrational spectra of NSAIDs, the molecular vibrations of OXA were analyzed [9–12]. The major vibrational modes of OXA were derived from those of carboxylic acid consisting of C=O, C–O, and O–H group and the vibrations of phenyl ring and CH_2 groups. Previously published detailed descriptions of the vibrations of the flurbiprofen dimer [10] were helpful in the identification of the cyclic carboxylic acid modes. The experimental Raman and FT-IR spectra of OXA are given in Figs. 4 and 5, respectively. The scaled fundamental frequencies, intensities of vibrational bands, and the form of vibrations obtained HF/6-31G(d) calculations together with the corresponding experimental bands and assignments for OXA are given in Table 4. The ν(OH), γ(OH. . .O) and ν(C=O) modes are generally characterized by HF/6-31G(d) level used as almost pure modes but other bands of OXA were generally coupled with vibrational bands of CH_2 group.

The molecules of carboxylic acids usually exist as centrosymmetric dimers in crystals with the centre of inversion within the eight-membered ring formed by two carboxyl groups [32]. The greatest difference in progressing from monomer to dimer is the changes in the frequencies of some peaks and COOH bands. The vibrations of the carboxylic group were studied as internal modes of the COOH group and intermolecular modes (COOH–HOOC). There were a lot of frequency shifts and a few new vibrations overall while processing from monomer to a dimer unit. Since the dimer is the larger molecule, lower frequency modes may be expected; and this appeared to be the case in this study.

Another important difference between the monomer and dimer is the appearance of the shifted lower frequency of OH-stretching band in the dimer. Since typical vibrational frequencies of free OH stretch bands were observed around 3600 cm^{-1}, the extremely low-frequency OH band observed for OXA indicated that the intermolecular hydrogen bond was formed. This mode as dimer form in KBr pellets gave rise to a very broad band between 2500 cm^{-1} and 3100 cm^{-1} [33] while in the IR spectrum of OXA, it was observed at 3056 cm^{-1} and calculated at 3038 cm^{-1}. Therefore, the OXA used in this study was in a dimeric form in the solid state. The OH symmetric mode was identified in observed FT-Raman spectrum; with the frequency at 3064 cm^{-1}.

The characteristic C=O stretch of the carboxyl group, on the other hand, appeared as a sharp peak in the 1680 cm^{-1} and 1725 cm^{-1} region. The strong absorption band at 1717 cm^{-1} may be assigned to C=O stretching mode while the corresponding transition in the IR spectrum of the flurbiprofen dimer appeared at 1701 cm^{-1} [10]. The observed band at 1723 cm^{-1} (Raman) and calculated at 1726 cm^{-1} was assigned as this mode of OXA dimer. Carboxylic dimers were absorbed in the region 955–915 cm^{-1} due to out-of-plane deformation of the carboxylic acid OH. . .O group [34]. It was assigned to this band at 921 cm^{-1} in the observed

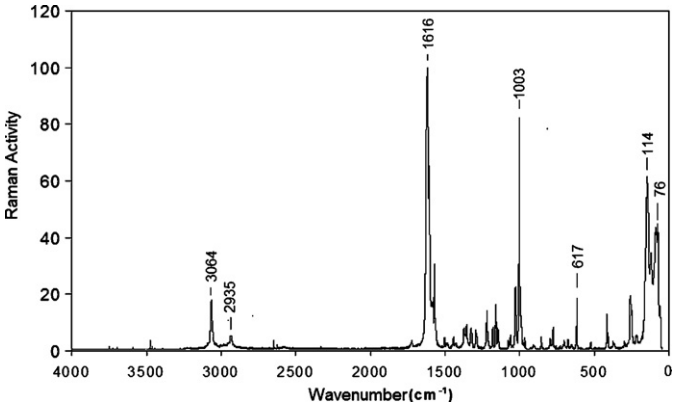

Fig. 4. FT-Raman spectrum of OXA dimer.

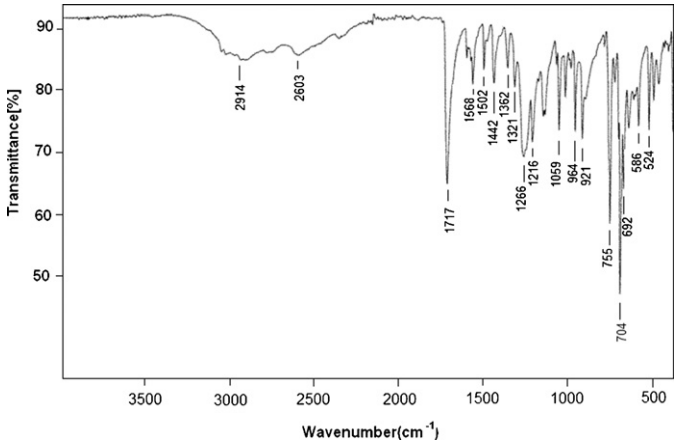

Fig. 5. FT-IR spectrum of OXA dimer.

Table 4
Comparison of the observed and calculated [HF/6-31G(d)] vibrational wavenumbers, IR intensities and Raman activities of oxaprozin dimer.

Assignments	Experimental		HF/6-31G(d)		IR intensities	Raman activities
	FT-IR	FT-Raman	Unscaled	Scaled		
ν(OH)	–	3064(vw)	3456	3076	–	556
ν(OH)	3056(vw)	–	3413	3038	976	–
$\nu(CH)_{RingA}$	3033(vw)	–	3378	3006	6	179
$\nu(CH)_{RingA}$	2978(vw)	–	3367	2997	8	153
$\nu(CH)_{RingB}$	2942(vw)	2935(vw)	3344	2976	14	108
$\nu(CH)_{RingA}$, $\nu_s(CH)_{RingB}$	2914(mw)	–	3341	2973	23	42
$\nu(CH)_2$	2790(w)	–	3178	2828	9	14
$\nu(CH)_2$	2764(vw)	–	3138	2793	4	38
$\nu(CH)_2$	2603(w)	2590(vw)	3000	2670	9	24
ν(C=O)	1717(s)	1723(vw)	1939	1726	878	57
$\nu(C_5–C_6)_{RingC}$	–	1616(vs)	1825	1624	–	1766
ν(C=N), $\nu(C–C)_{RingA}$	1605(vw)	1606(vw)	1796	1598	88	328
$\nu(C–C)_{RingB}$	1579(vw)	1580(vw)	1788	1591	15	17
$\nu(C–C)_{Rings}$	1568(mw)	1570(mw)	1736	1545	200	342
$\nu(C–C)_{Rings}$	1502(mw)	1505(vw)	1672	1488	37	20
$\delta(CH)_2$	1483(vw)	–	1636	1456	60	37
δ(CO), $\delta(CH_2)$	–	1445(vw)	1627	1448	–	36
δ(CO), $\delta(CH_2)$	1442(mw)	–	1599	1423	249	–
δ(COH), $\delta(CH)_2$	–	1372(vw)	1532	1363	–	31
ω(CH), ν(CC)	1362(w)	1355(w)	1515	1348	19	166
$\omega(CH_2)$	1321(vw)	1326(vw)	1463	1302	9	75
ω(CH)	–	1292(w)	1402	1248	–	68
$\omega(CH)_2$, δ(COH)	1266(mw)	–	1375	1197	449	–
ν(C–O), ν(C–N), $\delta(CCH)_{RingA}$	1216(w)	1220(w)	1328	1182	38	73
$t(CH_2)$	–	1181(vw)	1314	1169	–	20
ω(CH), $\delta(CC)_{Rings}$	1152(w)	1159(w)	1287	1145	1	23
ν(C–N)	1143(vw)	1145(vw)	1238	1102	4	44
δ(CCH), δ(CCC)	1076(vw)	1078(vw)	1164	1036	25	5
δ(CCC)	1060(w)	1063(vw)	1149	1023	33	7
δ(CCH), δ(CCC)	1023(mw)	1026(mw)	1143	1017	49	16
ω(CC)	–	1003(s)	1091	971	–	294
δ(C–O–C), τ(HCCH)	989(vw)	984(vw)	1066	949	67	8
$\tau(HCCH)_{Rings}$	964(w)	966(vw)	1053	937	58	27
γ(OH O)	921(w)	911(vw)	1024	912	381	–
$\rho(CH)_{ring}$	903(vw)	–	975	868	2	2
$\rho(CH)_{ring}$	–	856(w)	896	797	24	13
τ(HCCH)	791(vw)	796(vw)	888	790	51	2
$\delta(CH_2)$, γ(COC)	756(s)	776(w)	874	778	125	4
δ(CC), $\gamma(CH)_{Rings}$	729(vw)	–	814	725	41	9
δ(CH), $\gamma(CH)_{Rings}$	705(vw)	698(vw)	792	705	20	5
$(CH)_{Rings}$	693(vs)	–	787	700	142	–
δ(CCC)	675(w)	677(vw)	781	695	27	3
$\delta(CCC)_{Rings}$	646(w)	–	739	658	36	–
$\gamma(OCNC)_{RingC}$	616(vw)	617(mw)	748	645	20	15
τ(CCOH), γ(O=COH)	587(w)	–	685	610	150	–
$\gamma(CC)_{Rings}$	524(mw)	525(vw)	654	582	35	3
$\gamma(CC)_{Rings,}$ $\gamma(CH_2)$	496(w)	–	589	524	14	3
ρ(COOH), $\gamma(CC)_{rings}$	467(vw)	–	541	484	22	–
$\tau(CCCC)_{Rings}$	433(vw)	–	464	413	3	0
γ(CCC)	409(mw)	416(mw)	454	404	9	6
γ(skeletal)	–	367(vw)	407	362	–	6
$\gamma(CH_2)$	–	298(vw)	385	343	–	2
$\gamma(CH_2)$, τ(CCNC)	–	258(mw)	288	256	19	4
$\gamma_{(RingsA,B)}$	–	249(w)	274	244	20	12
ν(O...O)	–	222(vw)	263	234	–	7
τ(CCCC), $\gamma_{(Rings)}$	–	144(s)	253	225	–	3
ν(O...O)	–	122(m)	145	129	–	9
τ(Ph–Ph)	–	76(m)	81	72	–	10
τ(COOH), $\tau_{(Rings)}$	–	60(mw)	58	51	–	15

Vibrational modes: ν, stretching; δ, in-plane deformation; ω, wagging; γ, out-of-plane deformation; τ, torsion; ρ, rocking; s, strong; m, medium; w, weak; vw, very weak; sh, shoulder.

infrared spectrum of OXA. The theoretically calculated value at 912 cm^{-1} exactly coincided with the experimental value.

In the far-Raman spectrum of aspirin dimer, intermolecular O...O stretching mode occurs at 323 cm^{-1} and 130 cm^{-1}, respectively [20]. The theoretically predicted wavenumber, Raman scattering activity of the O...O stretching mode in OXA, was in good agreement with the experimental wavenumbers at 222 cm^{-1} and 122 cm^{-1} in the Raman spectrum, respectively, as can be seen in Table 4.

5. Conclusions

The geometric parameters, and electronic and optical properties of oxaprozin was calculated at the B3LYP/6-31G(d,p) and HF/6-31G(d,p) levels. The first calculated hyperpolarizabilities using HF/6-31G(d,p) and B3LYP/6-31G(d,p) levels were found as 1.029×10^{-30} and 1.117×10^{-30} esu, respectively. These values were found nearly six times more than that of urea (0.1947×10^{-30} esu) by using B3LYP/6-31G(d,p) level. A complete

vibrational study, accomplished through the analysis of the FT-IR and FT-Raman, were also compared with the vibrational spectra, obtained from HF/6-31G(d) level, as a dimer for the first time.

Acknowledgement

The authors would like to thank Kocaeli University Research Fund for its financial support (Grant No. 2009/007).

References

[1] M.A. al-Faks, M.C. Pugh, Orthop. Rev. 21 (5) (1992) 558–560.
[2] J.J. Talley, D.L. Brown, J.S. Carter, M.J. Graneto, C.M. Koboldt, J.L. Masferrer, W.E. Perkins, Y.Y. Zhang, K. Seibert, J. Med. Chem. 43 (2000) 775.
[3] K.D. Rainsford, H. Omar, A. Ashraf, A.T. Hewson, R.A.D. Bunning, R. Rishiraj, P. Shepherd, R.W. Seabrook, Inflammopharmacology 10 (3) (2002) 185–239.
[4] P.L. Franzen, S.C. Zilio, A.E.H. Machado, J.M. Madurro, A.G. Brito-Madurro, L.T. Ueno, R.N. Sampaio, N.M. Barbosa Neto, J. Mol. Struct. 892 (2008) 254–260.
[5] K.M. Nalin de Silva, J. Mol. Struct. THEOCHEM 725 (2005) 243–246.
[6] A. Hinchliffe, H.J. Soscun, Chem. Phys. Lett. 412 (2005) 365–368.
[7] T.M. Kolev, D.Y. Yancheva, B.A. Stamboliyska, M.D. Dimitrov, R. Wortmann, Chem. Phys. 348 (2008) 45–52.
[8] I.M. Kenawi, A.H. Kamel, R.H. Hilal, J. Mol. Struct. THEOCHEM 851 (2008) 46–53.
[9] S. Haman Bayari, S. Sagdinc, Struct. Chem. 19 (2008) 381–390.
[10] S. Sagdinc, H. Pir, Spectrochim. Acta Part A 73 (2009) 181–194.
[11] A. Jubert, N.E. Massa, L. Tevez, N.B. Okulik, J. Mol. Struct. 783 (1–3) (2006) 34–51.
[12] A. Jubert, N.E. Massa, L.T. Lopez, N.B. Okulik, Vib. Spectrosc. 37 (2005) 161–178.
[13] A.D. Becke, J. Chem. Phys. 98 (1993) 5648.
[14] C. Lee, W. Yang, R.G. Parr, Phys. Rev. B 37 (1988) 785.
[15] J.B. Foresman, A. Frisch, Exploring Chemistry with Electronic Structure Methods, Gaussian, Inc., Pittsburgh, PA, 1996, p. 64.
[16] M.J. Frisch, G.W. Trucks, H.B. Schlegel, G.E. Scuseria, M.A. Robb, J.R. Cheeseman, J.A. Montgomery Jr., T. Vreven, K.N. Kudin, J.C. Burant, J.M. Millam, S.S. Iyengar, J. Tomasi, V. Barone, B. Mennucci, M. Cossi, G. Scalmani, N. Rega, G.A. Petersson, H. Nakatsuji, M. Hada, M. Ehara, K. Toyota, R. Fukuda, J. Hasegawa, M. Ishida, T. Nakajima, Y. Honda, O. Kitao, H. Nakai, M. Klene, X. Li, J.E. Knox, H.P. Hratchian, J.B. Cross, V. Bakken, C. Adamo, J. Jaramillo, R. Gomperts, R.E. Stratmann, O. Yazyev, A.J. Austin, R. Cammi, C. Pomelli, J.W. Ochterski, P.Y. Ayala, K. Morokuma, G.A. Voth, P. Salvador, J.J. Dannenberg, V.G. Zakrzewski, S. Dapprich, A.D. Daniels, M.C. Strain, O. Farkas, D.K. Malick, A.D. Rabuck, K. Raghavachari, J.B. Foresman, J.V. Ortiz, Q. Cui, A.G. Baboul, S. Clifford, J. Cioslowski, B.B. Stefanov, G. Liu, A. Liashenko, P. Piskorz, I. Komaromi, R.L. Martin, D.J. Fox, T. Keith, M.A. Al-Laham, C.Y. Peng, A. Nanayakkara, M. Challacombe, P.M.W. Gill, B. Johnson, W. Chen, M.W. Wong, C. Gonzalez, J.A. Pople, Gaussian 03, Revision B.05, Gaussian, Inc., Wallingford CT, 2004.
[17] A. Frisch, A.B. Nielsen, A.J. Holder, GaussView Users Manual, Gaussian Inc., Pittsburg, 2000.
[18] A. Ben Ahmed, H. Feki, Y. Abid, H. Boughzala, A. Mlayah, J. Mol. Struct. 888 (2008) 180–186.
[19] D.S. Wishart, C. Knox, A.C. Guo, D. Cheng, S. Shrivastava, D. Tzur, B. Gautam, M. Hassanali, DrugBank: a knowledgebase for drugs, drug actions and drug targets, Nucleic Acids Res. 36 (January (Database issue)) (2008) D901–D906.
[20] M. Boczar, M.J. Wojcik, K. Szczeponek, D. Jamroz, A. Zieba, B. Kawalek, Chem. Phys. 286 (2003) 63.
[21] J.L. Flippen, R.D. Gilardi, Acta Crystallogr. Sect. B 31 (1975) 926–928.
[22] R.S. Mulliken, J. Chem. Phys. 23 (1955) 1833–1840.
[23] D.A. Kleinman, Phys. Rev. 126 (1962) 1977.
[24] Alan Hinchliffe, Beatrice Nikolaidi, J. Humberto, Soscún Machado, Int. J. Mol. Sci. 5 (2004) 224–238.
[25] C. Lin, K. Wu, Chem. Phys. Lett. 321 (2000) 83–88.
[26] A.D. Buckingham, in: B. Pullman (Ed.), Intermolecular Interactions: From Diatomics to Biopolymers, vol. I, Wiley, New York, 1978, p. 1.
[27] V. Krishnakumar, R. Nagalakshmi, Physica B 403 (2008) 1863–1869.
[28] D. Sajan, J.P. Abraham, I. Hubert Joe, V.S. Jayakumar, J. Aubard, O.F. Nielsen, J. Mol. Struct. 889 (2008) 129–143.
[29] J.P. Abraham, D. Sajan, I. Hubert Joe, V.S. Jayakumar, Spectrochim. Acta Part A 71 (2008) 355–367.
[30] D. Sajan, H. Joe, V.S. Jayakumar, J. Zaleski, J. Mol. Struct. 785 (2006) 43–53.
[31] D. Sajan, J. Binoy, I.H. Joe, V.S. Jayakumar, J. Zaleski, J. Raman Spectrosc. 36 (2005) 221.
[32] A.T. Dubis, S.J. Grabowski, D.B. Romanowska, T. Misiaszek, J. Leszczynski, J. Phys. Chem. A 106 (44) (2002) 10613–10621.
[33] N.B. Colthup, L.H. Daly, S.E. Wieberly, Introduction to Infrared and Raman Spectroscopy, Academic Press, USA, 1990.
[34] G. Socrates, Infrared and Raman Characteristic Group Frequencies: Tables and Charts, 3rd ed., 2004.